DALTON
FULL PAPER

Tuning of the transition metal hydrogen bond: how do *trans* ligands influence bond strength and hydridicity? †

Heiko Jacobsen ‡ and Heinz Berke

Anorganisch-chemisches Institut der Universität Zürich, Winterthurerstrasse 190, CH-8057 Zürich, Switzerland

Received 4th December 2001, Accepted 24th May 2002
First published as an Advance Article on the web 19th July 2002

Density functional calculations using the BP86, BLYP and PW91 functionals have been performed for the complexes $W(dmpe)_2H(X)$ (dmpe = $(CH_3)_2PCH_2CH_2P(CH_3)_2$); with X = ≡CH, **I**; NO, **II**; ≡N, **III**; ≡CMes (Mes = 2,4,6-$(CH_3)_3C_6H_2$), **Ia**; ≡CPh, **Ib**; ≡CMe, **Ic**; and ≡C*t*Bu, **Id**. The W–H bond strength increases in the order **III** < **I** < **II**, with an approximate difference of 20 kJ mol^{-1} between each pair. A perturbational analysis relates this effect to a variation in energy of the metal fragment orbital involved in bonding. The polarization of the W–H bond increases in the order **III** < **I** < **II**. The different functionals produce bond energy terms which differ in the range of about 8 kJ mol^{-1}, BP86 predicting the stronger, and PW91 the weaker bonds. The optimized geometric parameters are similar for all three functionals, with the exception of the W–P bonds, which are calculated to be about 4 pm longer with the BLYP approach. Bulkier carbyne ligands influence the coordination geometry of the dmpe ligands due to steric effects, which in turn influences the unit energy of the metal fragment orbital and thus the orbital interaction energy of the W–H (secondary *trans* influence).

Introduction

Transition metal hydrides[1] (TMH) play a prominent role in many transformations in the field of organometallic chemistry, in particular in homogeneous catalysis.[2–4] One important parameter is the strength of the M–H bond, which represents the key to catalysis.[5] Not only the thermodynamics of this bond, but also the bond polarity is of importance, since it has a direct influence on the kinetic preference of TMHs.

Within this context, our group has developed and investigated a series of Group VI TMH complexes of the type $W(CO)_nH(PR_3)_{4-n}(X)$. Here, R stands for an alkyl or alkoxy group, whereas X represents an activating ligand in *trans* position to the hydride. We have explored in detail the group of nitrosyl substituted hydride complexes, X = NO, which turned out to be an activated class of compounds.[6] Our initial studies were based on systems of the type $W(CO)_2H(NO)(PR_3)_2$, containing phosphorus donor ligands which may span a range of weak and strong σ-donors. Typical examples are complexes with the ligands triisopropylphosphite[7–10] or trimethylphosphine,[11–16] respectively. We then investigated the influence of different transition metal centers, synthesizing the corresponding chromium complexes[17] with phosphorus donor ligands, preparing the trisphosphine substituted derivatives.[18–20] Recently, we introduced the carbyne group ≡CMes (Mes = 2,4,6-$(CH_3)_3C_6H_2$) as an activating *trans* ligand[21,22] and observed a further increase in reactivity of this type of complex.

In the present study, we present a theoretical analysis of the influence of the *trans* ligand on the nature of the TMH bond. Calculations were performed on a series of compounds of the type $W(dmpe)_2H(X)$ (dmpe = $(CH_3)_2PCH_2CH_2P(CH_3)_2$); with X = ≡CH, **I**; NO, **II**; ≡N, **III**; ≡CMes, **Ia**; ≡CPh, **Ib**; ≡CMe, **Ic**; and ≡C*t*Bu, **Id**. We are not only interested in variations of the M–H bond strength, but also in the possibility of tuning the hydridic character of this bond. High level density functional calculations[23–26] are employed in order to get reliable thermodynamic and structural data, which then are connected to basic bonding principles and the requirement of a realistic modeling of the phosphine ligands, a point which is not given major consideration in recent review and other articles dealing with calculations on TMHs.[27,28] Several studies[29–32] revealed the fact that the commonly employed model phosphine PH_3 is in many cases well suited for studying geometries, but has severe shortcomings in the description of the electronic structure at the TM center, particularly when the electronics are dominated by σ-donating ligands. Although valuable insights can be obtained from a careful analysis of the chemical bond in model transition metal carbene complexes,[33] systems having the central metal in a phosphine rich environment require a more sophisticated description of the transition metal coordination sphere. A further aspect of the study on hand will include the investigation of different density functionals, which are advocated in the literature. We will compare the results of our computational studies with the structure and reactivity of the tungsten carbyne hydride W(≡CMes)$(dmpe)_2$H **1**, which we recently described,[22] and draw conclusions for the reactivity of the related hydrides $W(dmpe)_2H(NO)$ **2**, and $W(dmpe)_2H(≡N)$ **3**.

Results and discussion

We begin our discussion with a comparative analysis of the nature of the hydride ligand for optimized structures of complexes **I**–**III**, depicted in Scheme 1.

In this context, we will also judge the performance of the BP86 functional,[34,35] the first successful gradient-corrected density functional approach, in comparison with the BLYP[36] and PW91[37] methods.

Structural aspects

Selected geometric parameters for the optimized complexes **I**–**III** are compiled in Table 1.

† Electronic supplementary information (ESI) available: optimized geometries and bonding energies. See http://www.rsc.org/suppdata/dt/b1/b111085n/

‡ Current address: KemKom, 1864 Burfield Ave, Ottawa, ON, Canada K1J 6T1.

This journal is © The Royal Society of Chemistry 2002

Table 1 C_2-symmetric geometries[a] for complexes **I**, **II** and **III**, optimized by different density functionals

	I			**II**			**III**		
	BP86	BLYP	PW91	BP86	BLYP	PW91	BP86	BLYP	PW91
d(W–H)	190	192	190	184	186	185	199	201	199
d(W–P)	244	248	244	244	248	244	245 246	250	245 246
d(W–C)	185	186	185	—	—	—	—	—	—
d(W–N)	—	—	—	186	187	186	178	179	178
d(N–O)	—	—	—	122	123	121	—	—	—
∠(P–W–H)	81.4	81.9	81.5	82.3	83.2	82.4	81.2	82.3	81.4
∠(P–W–P)[b]	83.6	84.2	83.6	84.0	84.8	84.0	84.0	85.0	84.1

[a] Distances in pm, angles in °. [b] Bite angle of the dmpe ligand.

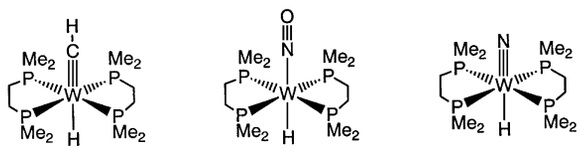

I **II** **III**

Scheme 1

Comparing the three DFT approaches employed in this study, we find as a noticeable difference that the BLYP method results in somewhat longer metal–ligand bond distances, which is most prominent for the W–P separation. Calculations with the BP86 and PW91 functionals lead to W–P distances around 244 pm, whereas the corresponding BLYP optimized bonds lengths are about 4 pm longer. However, the main structural picture obtained with the different methods is essentially the same. The carbon–tungsten triple bond has a length of 185 pm, virtually identical to that of the W–(NO) bond. The tungsten nitride triple bond is calculated to be significantly shorter by 7 pm. The coordination geometry of the carbyne and phosphine ligand in **I** might be compared with the crystal structure of the related molecule W(CH)(dmpe)$_2$(*n*Bu).[38] Here, the W–C bond amounts to 182.7(5) pm, being somewhat shorter than our calculated value, whereas the computed W–P distance of 244 pm lies well in the range of experimentally observed W–P separations, between 243.6(2) and 245.2(1) pm. The authors further report that the methylidyne unit is bent with an H–C–W angle of 162.3(39)°, and thus suggest that the *trans* influence of the *n*-butyl group might be responsible for this distortion.

The calculated W–H bond lengths increase in the order **II** < **I** < **III**, the nitrosyl complexes having the shortest, and the nitrido complex the longest TM–H bond, and span a range from 184 to 199 pm. This structural feature might be a first indication for the significant difference in *trans* influence exhibited by the ≡CR, NO, and ≡N ligands. In the next sections, we will discuss this aspect in greater detail.

Bond analysis

To this end, we make use of a well-established bond partitioning scheme,[39] which breaks down the bond between two fragments into various contributions from different interactions. In particular, we look at the bond-forming reaction between the atomic hydrogen fragment with the transition metal moieties W(dmpe)$_2$L^{trans}, L^{trans} being a carbyne, nitrosyl, or nitrido group. The energy associated with reaction 1 is called the bond snapping energy BE_{snap}. It can be partitioned into three main components, namely the electrostatic interaction ΔE_{elstat}, the Pauli repulsion ΔE_{Pauli}, and the orbital interaction term, ΔE_{int}.

$$BE_{snap} = -[\Delta E_{elstat} + \Delta E_{Pauli} + \Delta E_{int}] \quad (1)$$

When two suitable, bond forming fragments are brought together to adapt the geometry of the final molecule, the term ΔE_{elstat} describes the classical Coulomb interaction between the unmodified and interpenetrating charge distributions of the two fragments. We further have to consider the Pauli repulsion ΔE_{Pauli}, which takes into account destabilizing two-orbital four-electron interactions between occupied orbitals on both fragments. ΔE_{elstat} and ΔE_{Pauli} are often combined to yield the steric interaction term ΔE^0.

$$\Delta E^0 = \Delta E_{elstat} + \Delta E_{Pauli} \quad (2)$$

The last term in eqn. (1), ΔE_{int} introduces the attractive orbital interaction between occupied and virtual orbitals on the two fragments, and includes polarization and charge-transfer contributions.

Although BE_{snap} values are not defined in the same way as bond dissociation enthalpies ΔH, they are reasonable approximations of bond enthalpy terms, which in turn provide a good description for the bond strength.[5] A better approximation to ΔH is given by the bond energy BE. Since the equilibrium geometry of the W(dmpe)$_2$X fragments usually differs from their arrangement in the final molecule, a geometric preparation energy ΔE_{prep} is needed to get the fragments ready for bonding. Correcting BE_{snap} for this contribution, we obtain the bond energy as

$$BE = |BE_{snap}| - |\Delta E_{prep}| \quad (3)$$

The bonding analysis for complexes **I**–**III** is presented in Table 2.

Again, the results obtained from all three DFT methods are in good agreement, and give similar values for BE_{snap}. If we look at the electrostatic interaction, we see that the BLYP calculations produce a value, which is about 10 kJ mol^{-1} smaller compared to BP86 or PW91. Since the contributions to ΔE_{elstat} have a 1/*r* dependency, the slightly longer W–H bond for the BLYP optimized molecules causes the somewhat reduced electrostatic interaction. The values for ΔE_{elstat} obtained by the PW91 and BP86 methods are identical. These two approaches differ in that PW91 results in a slightly larger destabilization due to ΔE_{Pauli} and a weaker bonding orbital interaction ΔE_{int}. However, the difference in BE_{snap} obtained from BP86 and PW91 calculations is less than 10 kJ mol^{-1}, and all functionals employed in this study can be expected to give results of comparable quality for the class of molecules under investigation. Thus, for the remainder of the work, we will only work with the BP86 functional.

After having established our computational methodology, we next turn to a comparison of the systems with different *trans* ligands. Our calculations show that the W–H bond strength increases in the order **III** < **I** < **II**, with an approximate difference of 20 kJ mol^{-1} between each pair. An inspection of the data in Table 2 reveals some more noticeable details. First, we should mention that for all compounds, the steric interaction term ΔE^0 is dominated by the electrostatic interaction, and thus represents a bonding contribution. Further, we see that the

Table 2 Bond analysis[a] of the [W]–H bond for complexes **I**, **II** and **III**, using various density functionals

	I			**II**			**III**		
	BP86	BLYP	PW91	BP86	BLYP	PW91	BP86	BLYP	PW91
$\Delta E_{\mathrm{Pauli}}$	188	186	192	198	198	203	174	172	180
$\Delta E_{\mathrm{elstat}}$	−220	−208	−219	−239	−230	−239	−189	−179	−189
$\Delta E^{\mathbf{0}}$	−32	−22	−27	−41	−32	−36	−15	−7	−9
ΔE_{int}	−291	−294	−288	−305	−310	−303	−282	−286	−279
$\mathrm{BE}_{\mathrm{snap}}$	−323	−317	−316	−347	−342	−339	−297	−293	−288
ΔE_{prep}	11			11			15	—	—
BE	312			336			282		

[a] In kJ mol^{-1}.

Table 3 BP86 Voronoi charges[a] q^{V}, Mulliken charges[a] q^{M}, and Hirshfeld charges[a] q^{H} for the tungsten hydrides **I** to **III**

	I, L^{trans} = CH			**II**, L^{trans} = NO			**III**, L^{trans} = N		
	q^{V}	q^{M}	q^{H}	q^{V}	q^{M}	q^{H}	q^{V}	q^{M}	q^{H}
W	1.82	1.51	−0.03	1.86	1.36	−0.02	1.90	1.44	0.05
H	−0.99	−0.39	−0.18	−1.04	−0.39	−0.17	−0.95	−0.41	−0.21
L^{trans}	−0.88	−0.56	−0.22	−0.93	−0.48	−0.27	−1.13	−0.65	−0.37

[a] In u.

increase in bond strength is not only caused by an enhanced orbital interaction, but that the contribution from $\Delta E^{\mathbf{0}}$ plays an equally important role.

The correction due to the preparation energy lies between 10 and 15 kJ mol^{-1}, and amount to 3–5% of $\mathrm{BE}_{\mathrm{snap}}$. The main structural change in the metal fragments under relaxation is shortening of the W–L^{trans} bond, by 3–4 pm.

As mentioned before, the results from the bond analysis suggests that the W–H in all three complexes is hydridic in character. A similar conclusion can also be drawn from a charge analysis. Here, we have chosen Voronoi charges[40] q^{V}, in order to compare the H-ligands in the three different molecules. Voronoi charges for each atom are obtained from an integration of the total nuclear and electronic charge density in its Voronoi cell, which is the region of space that is closer to that atom than to any other one. In a similar way, Voronoi charges for groups of atoms may also be defined. The q^{V} values for complexes **I**–**III** are given in Table 3.

The hydridic character of the W–H bond is apparent as in all cases the calculated q^{V} value for the hydride ligand lies around $1e^{-}$. We further observe that q^{V} for this ligand increases in the order **III** < **I** < **II**, which might be interpreted as an increasing polarization of the W–H bond. Thus, the *trans* influence not only manifests itself in an increase of the W–H bond strength, but also through a simultaneous enhancement of hydridicity. It is further interesting to note that in all cases the Voronoi charges for the metal center and the *trans* ligand are close to +2 and −1. In the complexes **I**–**III**, the ligands L^{trans} might therefore be regarded as CH^{-}, NO^{-}, and N^{-}, respectively. However, a caveat is in order. One should keep in mind that formal oxidation numbers and partial charges, obtained by quantum mechanical calculations, are both important, but fundamentally different concepts, which have their advantages as well as limitations. This point is under discussion,[41,42] and care should be taken when results obtained from these different approaches are compared to each other.

For the sake of comparison, Mulliken charges q^{V} are also included in Table 3. Whereas Voronoi charges are directly related to the electron density $\rho(\mathbf{r})$, Mulliken charges constitute probably the most familiar scheme, wherein charges are obtained from an orbital-based population analysis. We observe that also according to the Mulliken scheme, the metal center is associated with a positive charge, whereas the hydride ligand and the ligand in *trans* position are both calculated to carry a negative charge. Major differences are found in the absolute size of the charge values, which are definitely smaller in the Mulliken case. However, on the whole compounds **I**, **II**, and **III**, the latter being somewhat more negatively charged, do not easily allow the assignment of significant differences in the polar character of the W–H bond.

Another scheme for assigning atomic charges, which is also based on the electron density $\rho(\mathbf{r})$ rather than on molecular orbitals, was proposed by Hirshfeld.[43] The Hirshfeld charges q^{H} are closely related to the deformation density known from crystal structure analysis. The charge q^{H} for a particular molecular fragment is calculated as the integral of the total molecular charge density, weighted by the relative fraction of the initial density of that fragment in the total initial density. Thus, q^{H} defines the reorganization of charge taking place when the atomic fragments, placed on their appropriate positions in the molecule, interact to form the actual molecule. From the values reported in Table 3, we see that the transition metal center now carries almost no net charge at all, in comparison to the positively charged tungsten centers obtained in the previously mentioned schemes. The Hirshfeld analysis thus reflects the electronic influence of the four strong phosphorus σ-donors. We also observe that all hydride ligands are associated with negative q^{H} values, indicating charge flow from the transition metal center to the hydride, and increasing its hydridic character.

Perturbational analysis

As we have seen from our bond analysis the orbital interaction ΔE_{int} is one of the main factors determining the strength of the W–H bond. Qualitative molecular orbital considerations derived from perturbation theory provide a useful picture of how the tuning of the $\mathrm{L}_n\mathrm{M}$–H bond *via* variation in ΔE_{int} might be accomplished. In a first order approximation, one can view the W–H bond as the result of a σ-type interaction of an orbital of the $\mathrm{L}_n\mathrm{M}$–H fragment, which is dominated by metal-d_σ-contributions, with the 1s orbital of the hydrogen ligand. This interaction is illustrated in Scheme 2.

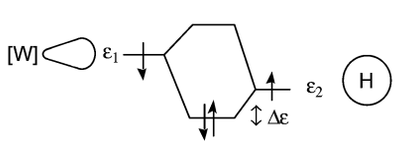

Scheme 2

To first order, the orbital stabilization $\Delta\varepsilon$ dpends on the difference $\Delta\varepsilon_0$ of the orbital energies of the bond forming fragments, as well as on their overlap S:

$$\Delta\varepsilon \approx S^2/|\varepsilon_1 - \varepsilon_2| \quad (4)$$

This expression tells us how a particular bond might be influenced. An increase in the overlap between the orbitals of both bonding partners should lead to a bond strengthening, while an increase in the energy gap between the interacting fragment orbitals causes the opposite effect.

The essential perturbational trend for our model compounds is summarized in Fig. 1.

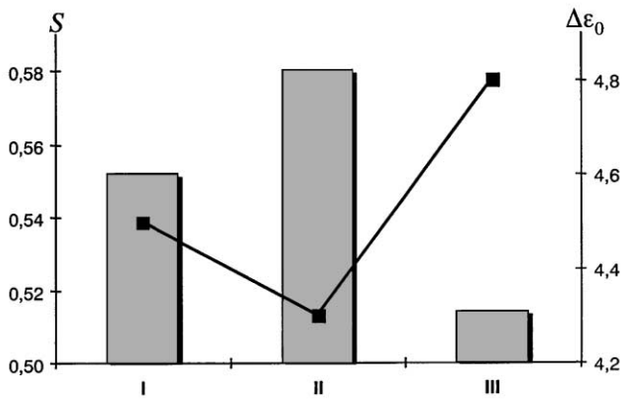

Fig. 1 Overlap integrals S (bars) and frontier orbital energy differences $\Delta\varepsilon_0$ (lines; in eV) for the L_nM–H bond in complexes **I**–**III**. The underlying values for ε_1 and ε_2 are those of the spin-restricted bond forming fragments.

The *trans* ligand has a strong influence on the orbital energy ε_1 of the transition metal fragment $W(dmpe)_2(X)$. The fragment with the strong π-accepting nitrosyl ligand has the lowest ε_1 value, followed by the carbyne and nitride systems. Thus, $\Delta\varepsilon_0$ for the fragments H and $W(dmpe)_2(X)$ increases as NO < CH < N, suggesting a decrease in the TM–H bond strength in the order NO > CH > N. The trend is paralleled by the values of the overlap integral S. This is understandable, since a stronger interaction causes a shorter metal–hydride bond, which in turn leads to an enhanced orbital overlap. Variation of the *trans* ligand therefore allows a tuning of the TM–H bond *via* the energy term ε_1 for the HOMO of the L_nM fragment. The change in S occurs as a consequence of the variation in $\Delta\varepsilon_0$ as a secondary effect. However, bond tuning *via* overlap variation can be achieved when the central metal is changed.[44] We should mention at this point that the correlation between hydrogen atom reactivities and valence orbital energies is a fairly established model, which has been successfully applied before to understand and predict hydridic or acidic behavior of TMHs.[45] Nevertheless, the pronounced influence of the *trans* ligand on the TM–H bond has not been demonstrated before. It is further worthwhile to note that our study indeed attributes a *trans* influence to both the nitrosyl as well as the nitrido ligand. In contrast, investigating the complexes $[OsCl_5(N)]_2$ and $[RuCl_5(NO)]_2^-$, Lyne and Mingos conclude that the nitrosyl group does not exhibit a *trans* influence on the chloride in opposite position.[46] When *trans* influence is defined as a weakening of the bond in question, their result is in accord with our study in the sense that the M–H bond is strongest in the nitrosyl complex **II**, which therefore might be set to zero on a relative scale.

Variation of the carbyne ligand

As already pointed out, introducing the mesitylcarbyne ligand ≡CMes as *trans* activating group dramatically enhances the reactivity of the corresponding tungsten hydrides. On the other hand, for the first representative of this class of compounds, namely the complex W(C*t*Bu)(H)(dmpe)$_2$ prepared by Schrock and co-workers,[47,48] it was stated that this compound does not react readily with small molecules[48] such as acetone. This prompted us to extend our theoretical study to include a series of carbyne substituted model compounds, W(CR)(H)(dmpe)$_2$, R = Mes, **Ia**, Ph, **Ib**, Me, **Ic**, and *t*Bu, **Id**, where **Ia** is identical with molecule **1**. These molecules are sketched in Scheme 3, and selected geometric parameters are collected in Table 4.

Table 4 Selected geometric parameters[a] for optimized BP86 geometries[a] for W(CR)(dmpe)$_2$H complexes **Ia**–**Id**

	Ia R = Mes	**Ib** R = Ph	**Ic** R = Me	**Id** R = *t*Bu
d(W–H)	189	190	190	189
d(W–P)	244	244	244	245
d(W–C)	189	187	186	187
∠(P–W–H)	79	81	81	80
	80	83	84	82

[a] Distances in pm, angles in °.

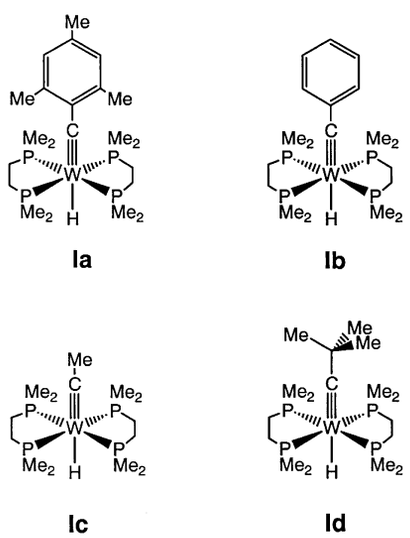

Scheme 3

We see that the bulkier carbyne ligands lead to an elongation of the W–C bond distance by a few pm, and to a decrease of the P–W–H angle by a few degrees. This angular distortion then has an influence on the [W]–H interaction energy, and might be classified as secondary *trans* influence. A basic exercise in five-coordination tells us the angular dependence on the orbital interaction energy for the TM–H bond.[49] As shown in Scheme 4,

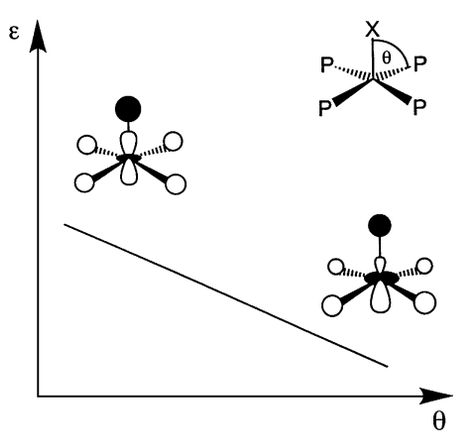

Scheme 4

Table 5 BP86 Bond energy terms[a] for the [W]–H bond in W(CR)-(dmpe)$_2$H complexes **Ia**–**Id**

	Ia R = Mes	**Ib** R = Ph	**Ic** R = Me	**Id** R = *t*Bu
ΔE^0	−24	−32	−33	−28
ΔE_{int}	−297	−294	−291	−295
BE_{snap}	321	326	321	323

[a] In kJ mol^{-1}.

an increase in the basal-apical angle lowers the energy of the d_{z^2}-based fragment orbital, which lowers the orbital energy gap $\Delta\varepsilon_0$ and consequently leads to a stronger orbital interaction.

This conclusion is corroborated by the trends observed in the ΔE_{int} values, which are reported in Table 5, together with values for ΔE_0 and BE_{snap}.

For the mesitylcarbyne complex **1a** with an average angle of pyramidalization θ_{av} of 101° we find a ΔE_{int} value of −297 kJ mol^{-1}, 6 kJ mol^{-1} higher than the ΔE_{int} contribution determined for **1** with θ_{av} = 97°. One has to keep in mind, however, that orbital interaction constitutes only one of the components of the [W]–H bond. Inspection of the ΔE_0 values in Table 5 shows that here the trend is contrary to that of ΔE_{int}, and as a result the bond snapping energies determined for all carbyne species are comparable, and do not follow any observed structural trend. The crystal structure of complex **1** has been determined before,[22] and its molecular geometry might be compared to the calculated structure of **Ia**, as shown in Fig. 2.

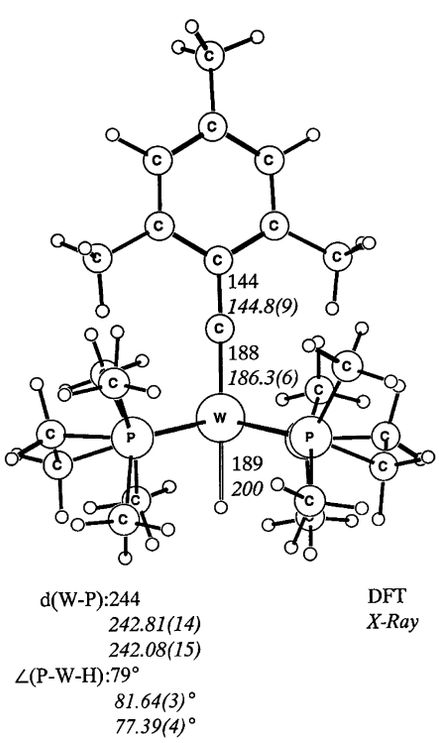

Fig. 2 The optimized BP86 geometry of complex **Ia**, in comparison with the X-ray crystal structure of **1**.

In general, the agreement between the results of the X-ray study and the BP86 calculations is quite satisfactory. As observed before, the calculations result in a somewhat longer W–C bond by about 2 pm. A major discrepancy, however, is observed for the metal–hydride distance. In the X-ray diffraction study, an unusually long W–H separation of 200 pm is found, whereas the calculated bond length is about 10 pm shorter. Although TM–H bond distances obtained from X-ray diffraction experiments should be interpreted with caution, the general trend is apparent. When comparing d_{W-H} for **1** with the value of 193 pm obtained for a related nitrosyl complex W(CO)H(PR$_3$)$_3$(NO),[20] it becomes clear that the more activated character of the metal–hydride bond for the carbyne complex manifests itself in a bond elongation of about 7 pm. The trend in the change of d_{W-H}, although not the magnitude, is faithfully reproduced in the outcome of the BP86 calculations.

Conclusion

We briefly summarize the main results of our previous study. We have demonstrated how variation of the *trans* ligand in complexes of the type W(dmpe)$_2$H(X) allows for a tuning of the TM–H bond. The W–H bond strength increases in the order **III** < **I** < **II**, with an approximate difference of 20 kJ mol^{-1} between each pair. A perturbational analysis relates this effect to variation in energy of the metal fragment orbital involved in bonding. The polarization of the W–H bond increases in the order **III** < **I** < **II**. The different functionals produce bond energy terms which differ in the range of about 8 kJ mol^{-1}, BP86 predicting the stronger, and PW91 the weaker bonds. The optimized geometric parameters are similar for all three functionals, with the exception of the W–P bonds, which are calculated to be about 4 pm longer with the BLYP approach. From our analysis, we expect, compared to W(≡CMes)-(dmpe)$_2$H **1**, the nitrosyl compound[50] W(dmpe)$_2$H(NO) **2** to be more reactive in reactions governed by kinetic effects, whereas the hypothetical W(dmpe)$_2$H(≡N) **3** should be more reactive when thermodynamic effects are in control.

Computational methodology

All calculations have been performed with the ADF program package, version 2000.02.[40,50,51] The local exchange-correlation potential of Vosko and co-workers[52] was augmented self-consistently by Becke's exchange gradient-correction[34] and Perdew's correlation gradient-correction[35] (BP86), or by the exchange and correlation corrections proposed by Perdew and Wang[37] (PW91). Additionally, calculations utilizing the correlation functional of Lee, Yang and Parr,[36] together with Becke's exchange corrections, were carried out (BLYP). The ADF basis set IV (triple-ζ STO plus one polarization function) was used for W, N, O, as well as for the hydride H and carbyne C. Basis set III (double-ζ STO plus one polarization function) was employed for P, the C and H atoms of the aryl and alkyl groups of the carbyne ≡CR ligands, with the exception of the methyl groups on ≡CMes. The remaining atoms were described by basis set II (double-ζ STO). Relativistic effects have been included using a quasi-relativistic approach.[53–55] Within this scheme, it was prohibitive to use basis set IV for the phosphorus atoms, which led to variational collapse.[56] For complexes **I**, **Ib**, **II** and **III** C_2 symmetry was employed. Attempts to optimize geometries for complexes with a bent CH or NO ligand failed, essentially resulting in a linear arrangement. Optimized geometries and bonding energies are given in the supplementary material. †

References

1 *Transition Metal Hydrides*, ed. A. Dedieu, VCH, Weinheim, 1992.
2 *Catalytic Transition Metal Hydrides*, ed. D. W. Slocum and W. R. Moser, Annuals of the New York Academy of Sciences, New York, 1983, vol. 415.
3 *Applied Homogeneous Catalysis with Organometallic Compounds*, ed. B. Cornils and W. A. Herrmann, Wiley-VCH, Weinheim, 1999.
4 *Catalysis from A to Z*, ed. B. Cornils, W. A. Herrmann, R. Schlögl and C.-H. Wong, Wiley-VCH, Weinheim, 2000.
5 J. A. M. Simões and J. L. Beauchamp, *Chem. Rev.*, 1990, **90**, 629.
6 H. Berke and P. Burger, *Comments Inorg. Chem.*, 1994, **16**, 279.
7 P. Kundel and H. Berke, *J. Organomet. Chem.*, 1986, **314**, C31.
8 P. Kundel and H. Berke, *J. Organomet. Chem.*, 1987, **335**, 353.

9 P. Kundel and H. Berke, *Z. Naturforsch., Teil B*, 1987, **42**, 993.
10 P. Kundel and H. Berke, *J. Organomet. Chem.*, 1988, **339**, 297.
11 A. A. H. van der Zeijden, V. Shklover and H. Berke, *Inorg. Chem.*, 1991, **30**, 4393.
12 A. A. H. van der Zeijden, C. Sontag, H. W. Bosch, V. Shklover, H. Berke, D. Nanz and W. von Philipsborn, *Helv. Chim. Acta*, 1991, **74**, 1194.
13 A. A. H. van der Zeijden and H. Berke, *Helv. Chim. Acta*, 1992, **75**, 513.
14 A. A. H. van der Zeijden, H. W. Bosch and H. Berke, *Organometallics*, 1992, **11**, 2051.
15 A. A. H. van der Zeijden, H. W. Bosch and H. Berke, *Organometallics*, 1992, **1**, 563.
16 A. A. H. van der Zeijden, D. Veghini and H. Berke, *Inorg. Chem.*, 1992, **31**, 5106.
17 A. A. H. van der Zeijden, T. Bürgi and H. Berke, *Inorg. Chim. Acta*, 1992, **201**, 131.
18 F. P. Liang, H. Jacobsen, H. W. Schmalle, T. Fox and H. Berke, *Organometallics*, 2000, **19**, 1950.
19 F. Bäth, Ph. D. Thesis, University of Zürich, Zürich, 1998.
20 J. Höck, H. Jacobsen, H. W. Schmalle, G. Artus, T. Fox, J. I. Amor, F. Bäth and H. Berke, *Organometallics*, 2001, **20**, 1533.
21 E. Bannwart, H. Jacobsen, F. Furno and H. Berke, *Organometallics*, 2000, **19**, 3605.
22 F. Furno, T. Fox, H. W. Schmalle and H. Berke, *Organometallics*, 2000, **19**, 3620.
23 T. Ziegler, *Chem. Rev.*, 1991, **91**, 651.
24 W. Kohn, A. D. Becke and R. G. Parr, *J. Phys. Chem.*, 1996, **100**, 12974.
25 E. J. Baerends and O. V. Gritsenko, *J. Phys. Chem. A*, 1997, **101**, 5383.
26 W. Koch and M. C. Holthausen, *A Chemist's Guide to Density Functional Theory*, Wiley-VCH, Weinheim, 2000.
27 D. K. Seo, G. Papoian and R. Hoffmann, *Int. J. Quantum Chem.*, 2000, **77**, 408.
28 F. Maseras, A. Lledos, E. Clot and O. Eisenstein, *Chem. Rev.*, 2000, **100**, 601.
29 H. Jacobsen and H. Berke, *Chem.-Eur. J.*, 1997, **3**, 881.
30 O. Gonzalez-Blanco and V. Branchadell, *Organometallics*, 1997, **16**, 5556.
31 T. Hascall, D. Rabinovich, V. J. Murphy, M. D. Beachy, R. A. Friesner and G. Parkin, *J. Am. Chem. Soc.*, 1999, **121**, 11402.
32 H. M. Senn, D. V. Deubel, P. E. Blöchl, A. Togni and G. Frenking, *THEOCHEM*, 2000, **506**, 233.
33 S. E. Vyboishchikov and G. Frenking, *Chem. Eur. J.*, 1998, **4**, 1439.
34 A. D. Becke, *Phys. Rev. A*, 1988, **38**, 3098.
35 J. P. Perdew, *Phys. Rev. B*, 1986, **33**, 8822.
36 C. T. Lee, W. T. Yang and R. G. Parr, *Phys. Rev. B*, 1988, **37**, 785.
37 J. P. Perdew and Y. Wang, *Phys. Rev. B*, 1992, **45**, 13244.
38 J. Manna, S. J. Geib and M. D. Hopkins, *Angew. Chem., Int. Ed. Engl.*, 1993, **32**, 858.
39 F. M. Bickelhaupt and E. J. Baerends, *Rev. Comput. Chem.*, 2000, **15**, 1.
40 G. te Velde and E. J. Baerends, *J. Comput. Phys.*, 1992, **99**, 84.
41 M. Kaupp and H. G. von Schnering, *Angew. Chem., Int. Ed. Engl.*, 1995, **34**, 986.
42 J. P. Snyders, *Angew. Chem., Int. Ed. Engl.*, 1995, **34**, 986.
43 F. L. Hirshfeld, *Theor. Chim. Acta*, 1977, **44**, 129.
44 H. Jacobsen and H. Berke, in *Recent Advances in Hydride Chemistry*, ed. R. Poli and M. Peruzzini, Elsevier, Amsterdam, 2001.
45 B. E. Bursten and M. G. Gatter, *Organometallics*, 1984, **3**, 895.
46 P. D. Lyne and D. M. P. Mingos, *J. Chem. Soc., Dalton Trans.*, 1995, 1635.
47 D. N. Clark and R. R. Schrock, *J. Am. Chem. Soc.*, 1978, **100**, 6774.
48 S. J. Holmes, D. N. Clark, H. W. Turner and R. R. Schrock, *J. Am. Chem. Soc.*, 1982, **104**, 6322.
49 A. R. Rossi and R. Hoffmann, *Inorg. Chem.*, 1975, **14**, 365.
50 E. J. Baerends, D. E. Ellis and P. Ros, *Chem. Phys.*, 1973, **2**, 41.
51 C. Fonseca Guerra, J. G. Snijders, G. te Velde and E. J. Baerends, *Theor. Chem. Acc.*, 1998, **99**, 391.
52 S. H. Vosko, L. Wilk and M. Nusair, *Can. J. Phys*, 1980, **58**, 1200.
53 J. G. Snijders, E. J. Baerends and P. Ros, *Mol. Phys.*, 1979, **38**, 1909.
54 T. Ziegler, J. G. Snijders and E. J. Baerends, *J. Chem. Phys.*, 1981, **74**, 1271.
55 T. Ziegler, V. Tschinke, E. J. Baerends, J. G. Snijders and W. Ravenek, *J. Phys. Chem.*, 1989, **93**, 3050.
56 E. van Lenthe, A. Ehlers and E. J. Baerends, *J. Chem. Phys.*, 1999, **110**, 8943.